Computational Study of Two-Dimensional Gravitational Rings Under Internal Time-Varying Repulsive Force

Kamyar Modjtahedzadeh[*]

www.spyderkam.com

November 22, 2025

Abstract

. . . To come. . .

---

[*]kam@spyderkam.com

Table of Contents

1 Introduction

…way off…

1.1 Inferiority of Euler Method to Velocity Verlet Integration

1.1.1 Simulation and Results of Euler Method

A square perimeter subject to the gravitational force between its own constructing point particles each with unit mass will be simulated over time using the Euler method. The structure will will start with 100 evenly space particles with the first particle located at $(x, y) = (0, 0)$ and the length of each side of the square is 1.

Parameters and Expectations   Using the Euler method, both simulations model pairwise gravitational interactions through Newton's law of universal gravitation:

$$\vec{F}_{\text{grav}} = -G \cdot \frac{m_1 m_2}{r^2} \hat{r}, \tag{1.1}$$

where G represents the gravitational field/attraction strength and is *not* a constant of simulation, albeit a constant of nature. The negative sign indicates that gravity is an attractive force.

Starting at $t_{\text{initial}} = 0$, the first simulation employs a very strong gravitational coupling of $G = 10^6$, timestep $\Delta t = 10^{-3}$, and runs for 10^3 steps spanning a total duration of $t_{\text{final}} = 1$. The second simulation drastically reduces the gravitational constant to $G = 10^2$ while also drastically reducing the timestep length to 5×10^{-6}, thus capturing the system at an earlier moment $t_{\text{final}} = 5 \times 10^{-3}$. Both systems should exhibit near-identical behavior: The point


(a) $G = 10^6$, $\Delta t = 10^{-3}$ (b) $G = 10^2$, $\Delta t = 5 \times 10^{-6}$
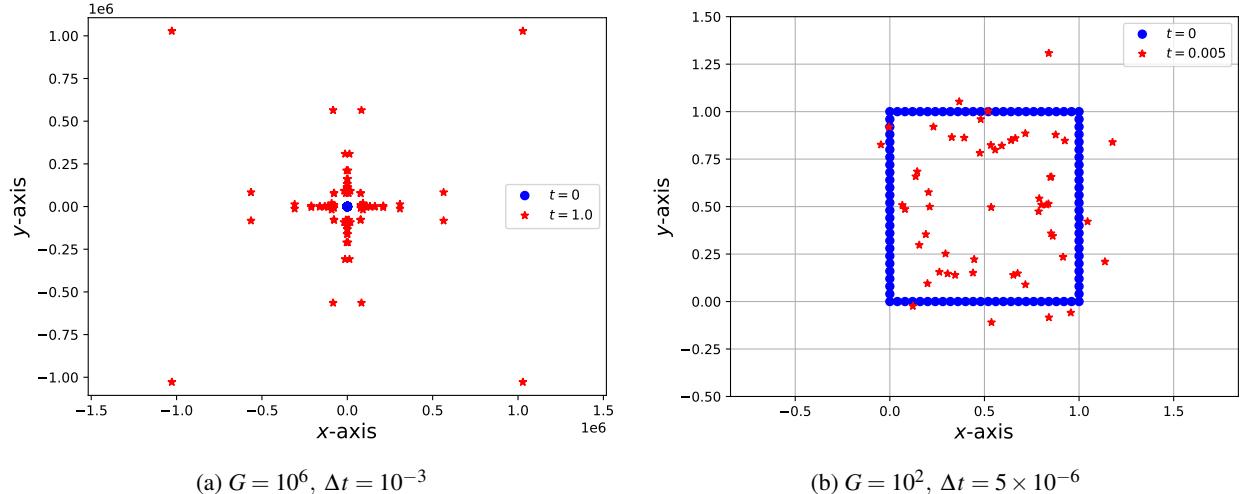
Figure 1.1: The Euler integration method applied to the same 2D shallow square of 100 particles over 1,000 timesteps. When Δt is *not* small enough, as in Figure 1.1a, the structure flies apart, something that is not expected under the attractive force in Equation (1.1). When Δt *is* small enough, as in Figure 1.1b, the system acts as closer to what is expected from it; that being said, over the same number of timesteps (i.e., iterations), a significantly smaller t_{final} is reached.

particles should accelerate inward and converge toward the structure's center of mass, forming a compact cluster. The conservation of energy in this isolated gravitational system dictates that particles initially at rest cannot acquire sufficient kinetic energy to overcome the gravitational potential well and escape.

Observations and Discrepancies   While a gravitational collapse may have occurred for a seemingly insubstantial fraction of the number of particles in the first simulation, the vast majority of particles have clearly moved far away from the center of mass of the structure's initial configuration, as shown in Figure 1.1a. A direct contradiction of the principle of energy conservation. On the other hand, operating under the same laws of physics, the second simulation, captured at the earlier time of $t = 0.005$ in Figure 1.1b, behaves as expected. The square structure has contracted substantially, with particles migrating inward toward the center of mass. Although a few particles have moved farther than expected, the overall picture depicts a collapsing structure consistent with gravitational theory.

1.1.2 Systematic Errors of the Euler Method

Numerical Error Accumulation   The difference between expected and observed behavior in the first simulation is due to systematic errors introduced by the The Euler method.[1] The Euler integration method represents a basic numerical approach for solving ordinary differential equations, updating particle velocities and positions according to the following equations:

$$\vec{a}_i(t) = \vec{F}_i(t)/m_i \tag{1.2}$$

$$\vec{v}_i(t+\Delta t) = \vec{v}_i(t) + \vec{a}_i(t)\Delta t \tag{1.3}$$

$$\vec{r}_i(t+\Delta t) = \vec{r}_i(t) + \vec{v}_i(t)\Delta t. \tag{1.4}$$

The issue with this method is that it treats continuously varying forces as piecewise constant values. At the beginning of each iteration, the method evaluates all forces based on current particle positions, computes accelerations, and then applies these accelerations uniformly throughout the entire duration of the timestep. This approximation fails to account for the fact that particles move *during* the timestep. The gravitational force's inverse-square dependence on distance causes the particles to approach one another, forces increase rapidly, and the assumption of constant acceleration over the timestep becomes increasingly inaccurate in this approximation. The Euler method's approximation errors introduce spurious energy into the system at each timestep. When a particle experiences a strong attractive force and accelerates toward another particle, the Euler method applies that force for the full timestep duration even as the particle moves closer and the actual force should be increasing. This delayed response to strengthening forces causes particles to acquire velocities that are systematically too large, effectively injecting kinetic energy that has no physical origin. One workaround is to use a very short timestep, but that would require tremendously more iterations and computational power to achieve a desired t_{final}. For the gravitational N-body problem, particularly when particles can approach closely and generate stiff dynamics through the inverse-square force law, the Euler integration method will eventually fail regardless of how small the timestep becomes, unless the timestep is reduced to impractically tiny values.

Symplectic Integration for Energy Conservation   The Euler method is simply inadequate for simulating conservative systems over long periods. The non-symplectic method's first-order accuracy makes it unsuitable for problems requiring energy conservation. One solution for such problems could be to adopt symplectic, higher-order integration schemes specifically designed for Hamiltonian systems. A symplectic integrator is a numerical method that accurately conserves important physical quantities over sufficiently large time scales. A crucial and necessary condition for standard, explicit integrators to work correctly on a specific class of conservative dynamical systems is *time reversibility*, something which the standard explicit Euler method is not (see Appendix A.2.1). For a time-reversible Hamiltonian system, Liouville's theorem asserts that the volume[2] occupied by a set of initial conditions in phase space is conserved over time.

   The Verlet integration method, for instance, is a second-order symplectic integrator that exhibits excellent long-term energy conservation properties. Symplectic integrators preserve the geometric structure of phase space and maintain bounded energy errors even over extremely long simulation times for conserved Hamiltonian systems.

1.2   Velocity Verlet Integration

In four stages per timestep, the velocity Verlet algorithm advances a particle system through discrete timesteps while maintaining time reversibility and symplectic structure.

1. The current acceleration is computed from the force acting on the particle: $\vec{a}(t) = \vec{F}(t)/m$.
2. The position is advanced using the current velocity and acceleration:

$$\vec{r}(t+\Delta t) = \vec{r}(t) + \vec{v}(t)\Delta t + \frac{1}{2}\vec{a}(t)\Delta t^2. \tag{1.5}$$

---

[1]**First-Order Accuracy:** The Euler method is called a first-order method because the error per step is proportional to the square of the step size (Δt^2), and the global error is proportional to the step size (Δt). This means that if the step size is halved, the error is also approximately halved. The method is linear in its error reduction with respect to the step size.

[2]Area in two dimensions.

3. Forces are recomputed at the new particle positions to obtain $\vec{F}(t+\Delta t)$, from which the new acceleration follows: $\vec{a}(t+\Delta t) = \vec{F}(t+\Delta t)/m$.

4. The velocity is updated using the average of the old and new accelerations:

$$\vec{v}(t+\Delta t) = \vec{v}(t) + \frac{1}{2}\left[\vec{a}(t) + \vec{a}(t+\Delta t)\right]\Delta t. \tag{1.6}$$

The velocity Verlet algorithm is a second-order method with local truncation error proportional to Δt^3 and global error proportional to Δt^2. This represents a significant improvement over the first-order Euler method, which has local error proportional to Δt^2 and global error proportional to Δt. (See Appendix B for more details.)

1.2.1 Early Performance Analysis: Stiff Gravitational Systems

The modified gravitational force between particles i and j is given by,

$$\vec{F}'_{\text{grav}} = -G \cdot \frac{m_i m_j}{r_{ij}^2 + \varepsilon_{\text{grav}}^2}\, \hat{r}_{ij} \tag{1.7}$$

where $\varepsilon_{\text{grav}}$ is a softening parameter that prevents numerical divergence at small separations. For strongly coupled gravitational systems with $G \geq 50$, testing reveals that over a long enough time before gravitational collapse, the velocity Verlet algorithm will preserve an organized structure while the Euler integration method produces a dispersed cluster collapse and focus around some focal point, as seen in Figure 1.2. Physically, this means that Verlet integration better preserves the system's dynamical invariants, as expected. The method has bounds to the energy error making particles follow more realistic orbits, some particles remain in quasi-periodic trajectories developing patterns which likely would not have analogous counterparts if the initial configuration was not a well defined shape such as a square.

(a) Velocity Verlet method   (b) Euler integration method
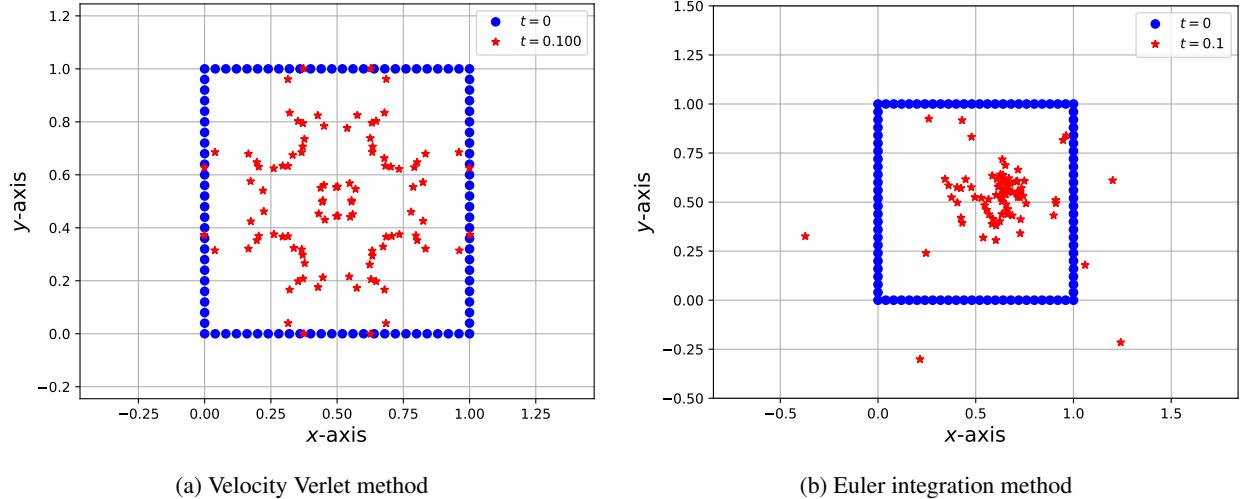
Figure 1.2: Gravitational collapse of a square perimeter made up of 100 unit-mass point particles using velocity Verlet and Euler integration methods. Both methods run over 10^4 iterations with $\Delta t = 10^{-5}$, $G = 10$, and $\varepsilon_{\text{grav}} = 0.05$. It is evident that the velocity Verlet integration has preserved phase space related quantities as it has maintained a structure. Figure 1.2b on the other hand is chaotic and indicates no preservation of such quantities. Figure 1.2a should also eventually collapse, before $\vec{F}'_{\text{grav}}$ eventually explodes, even with its softening parameter.

Euler integration on the other hand injects artificial energy into the system causing the particles to gain excessive kinetic energy and ultimately escape to infinity or collapse too aggressively resulting in a loss of structure. Despite the fact that this too ultimately happens with Verlet integration, it happens far earlier using the Euler method as the former method is more unstable. The previously mentioned "organized structure" is particles maintaining correlated motion rather than random scattering. This preservation of geometric structure allows the velocity Verlet integration to maintain a physically realistic so-called final configuration over longer timescales whereas the Euler method's energy drift dominates the dynamics.

1.2.2 Long-Term Velocity Verlet Numerical Instability

As previously mentioned, over long enough time scales, even the velocity Verlet method will fail with just Equation (1.7). For example, in Figure 1.2a, the point particles are expected to eventually gather into a singularity in the center where the square perimeter is initially located; however, the N-body system fragments before it fully collapses. The same behavior can be seen with a shallow circle; a uniform ring *should* collapse toward a point at the center. This is evident from a symmetry argument: all particles are pulled towards the symmetry center, and they fall toward it at the same rate.[3] Yet, this exact behavior is not recovered in the current model for the N-body configuration due to numerical artifacts.

(a) 8,000 iterations

(b) 10,000 iterations

(c) 12,000 iterations

(d) 50,000 iterations
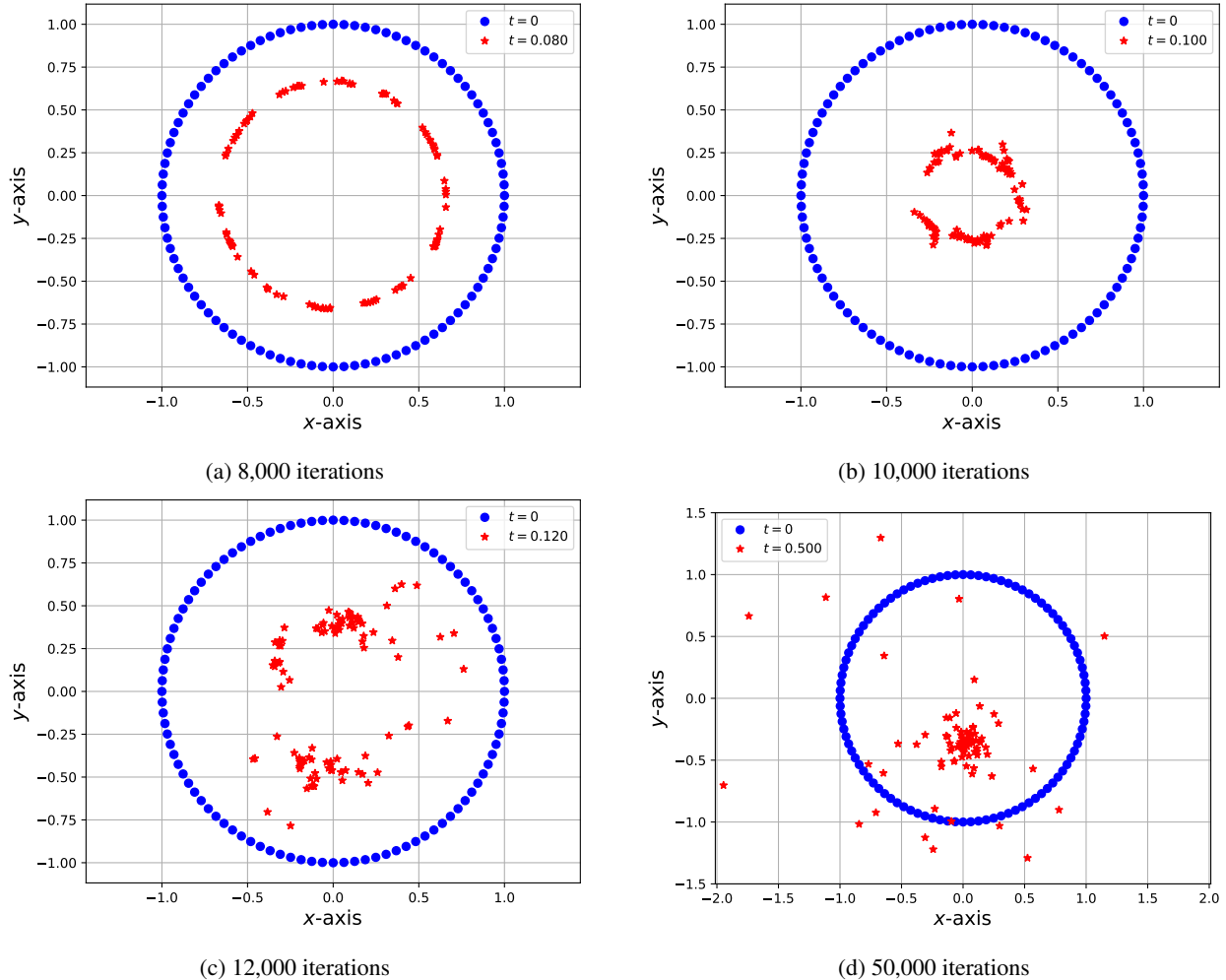
Figure 1.3: The initial configuration is a unit circle centered at the origin with otherwise all the parameters as those in Figure 1.2. The uniform ring is unstable; any region of above average density tends to attract more material over time. Even though the particles are initially equally spaced, small numerical artifacts cause some particles to end up slightly closer than others, and these small differences get amplified over time due, causing the structure to fragment before gravitational collapse.

---

[3]For more general shapes, the symmetry argument does not hold, and in general the particles should not collapse to a point.

2   Time-Varying Repulsive Force

To induce breathing oscillations in the *N*-body systems, a time-varying repulsive force is implemented alongside the gravitational attraction. This force models periodic oscillation of repulsion strength, creating expansion-contraction cycles.

$$\vec{F}_\zeta(t) = |k_\zeta| \cdot \frac{\zeta(t)}{r_{ij}^2 + \varepsilon_\zeta^2}\, \hat{r}_{ij}, \tag{2.1}$$

with $\zeta(t)$ being the modulating signal which follows a sinusoidal form:

$$\zeta(t) = 1 + \sin(\omega_\zeta t), \tag{2.2}$$

where ω_ζ is the angular frequency of pulsation.

2.1   *N*-Body Structure With Internal Modulating Repulsion Signal

Consider a system in a vacuum where the total force on each of its constructing particles is:

$$\vec{F}_{\text{total}}(t) = \vec{F}'_{\text{grav}} + \vec{F}_\zeta(t). \tag{2.3}$$

At the start of a simulation, $t_0 = 0 \Rightarrow \zeta(t_0) = 1$, at a later time $\omega_\zeta t = \pi/2 \Rightarrow \zeta(0.5\pi/\omega_\zeta) = 1$ where ζ and hence the modulating repulsive force are *increasing* from $t_0 \to \pi/(2\omega_\zeta)$. Again, let all $m = 1$, the numerators of equations (1.7) and (2.1) are then:

$$m_i m_j \Big|_{m=1} : \ 1, \,\overset{=}{\cdot}., 1, \,\overset{=}{\cdot}., 1, \,\overset{=}{\cdot}., 1, \,\overset{=}{\cdot}., 1, \,\overset{=}{\cdot}., 1, \,\overset{=}{\cdot}., 1 \dots \tag{2.4a}$$

$$\zeta(t) \qquad : \ \underbrace{1, \,\overset{\uparrow}{\cdot}., 2, \,\overset{\downarrow}{\cdot}., 1, \,\overset{\downarrow}{\cdot}., 0, \,\overset{\uparrow}{\cdot}., 1, \,\overset{\uparrow}{\cdot}., 2, \,\overset{\downarrow}{\cdot}., 1,}_{\text{one full period}} \dots \tag{2.4b}$$

The first "1" in line (2.4b) corresponds to t_0, "$\overset{\uparrow}{\cdot}.$" means that ζ is increasing until it hits $\zeta(0.5\pi/\omega_\zeta) = 2$, and then again decreasing until it hits $\zeta(0.75\pi/\omega_\zeta) = 1$, and so on.

To find an appropriate pulsation angular frequency, it is best to be priori known either the desired final time of simulation or the total number of iterations (n). As long as either one is known, the other one can easily be calculated using the formula $t_{\text{final}} = n\Delta t$.[4] Now, since $t_0 = 0$, a full period happens when the argument of the sine function in the expression for $\zeta(t)$ is 2π; i.e., $\omega_\zeta \tau = 2\pi$, where τ is the period. So if the simulation desires n timesteps to reach one full cycle then $\omega_\zeta = 2\pi/(n\Delta t)$. If the simulation desires to go through c cycles,

$$\omega_\zeta \Big|_c = \frac{2\pi c}{n\Delta t}. \tag{2.5}$$

2.2   Radial Stability Under Internal Sinusoidal Repulsive Forcing

Consider a test particle with unit mass at radius $R(t)$ from the system's center of mass. The *radial equation of motion* in the limit where softening is negligible ($\varepsilon \ll R$) becomes:

$$\frac{d^2 R}{dt^2} = -G \cdot \frac{M_{\text{eff}}}{R^2} + \lambda G \cdot \frac{\zeta(t)}{R^2}, \tag{2.6}$$

where λ is the gravitational scaling factor given from $|k_\zeta| = \lambda G$ and M_{enc} is the effective mass of all the other particles are initially placed at the same radius R_0, M_{eff} represents the effective mass contributing to the radial restoring force;

---

[4]Inverse manipulations can also be performed to obtain simulation parameters.

for a thin ring of identical particles, this is all the particles other than the test particle: $M_{\text{eff}} = (N-1)m$. For large N, $M_{\text{eff}} \approx Nm = M_{\text{total}}$.[5] Anyhow, Equation (2.6) simplifies to,

$$\frac{d^2R}{dt^2} = \frac{G}{R^2}\left[\lambda\zeta(t) - M_{\text{eff}}\right]. \tag{2.7}$$

For time-averaged equilibrium at $\langle R(t)\rangle = R_0$, as it will be shown, $\lambda \neq M_{\text{eff}}$, as the natural frequency derived and displayed later in Equation (2.19) becomes zero, eliminating the restoring force and making the system vulnerable to parametric resonance from the time-varying drive at ω_ζ. Although Equation (2.7) is not a Mathieu equation due to its nonlinearity,[6] the instability mechanism is analogous: When the natural frequency vanishes ($\omega_0 = 0$), the time-dependent repulsive coupling drives unbounded growth of radial perturbations—a hallmark of Mathieu-type parametric instability—which will emerge explicitly in the linearized, non-uniform case.

To verify this instability mechanism, linearize around R_0. Assume a small perturbation around equilibrium radius and let $R(t) = R_0 + \delta R(t)$ where the perturbation is always much smaller than the equilibrium radius. To linearize Equation (2.7), start by Taylor expanding $1/R^2$:

$$\frac{1}{R^2} = \frac{1}{(R_0 + \delta R)^2} = \frac{1}{R_0^2}\left(1 + \frac{\delta R}{R_0}\right)^{-2}, \tag{2.8}$$

since $|\delta R(t)| \ll R_0$, using $(1+z)^{-2} \simeq 1 - 2z$ yields,

$$\frac{1}{R^2} \simeq \frac{1}{R_0^2}\left(1 - \frac{2\delta R}{R_0}\right), \tag{2.9}$$

substituting this into Equation (2.7),

$$\frac{d^2}{dt^2}\delta R = \frac{G}{R_0^2}\left[\lambda\zeta(t) - M_{\text{eff}}\right]\left(1 - \frac{2\delta R}{R_0}\right). \tag{2.10}$$

For the expansion to be consistent around R_0, the zeroth-order terms (independent of δR) must vanish on average: $\langle\lambda\zeta(t) - M_{\text{eff}}\rangle = 0 \Rightarrow \lambda = M_{\text{eff}}$. However, this time-averaged balance does not guarantee stability, it produces $\omega_0^2 = 0$, leaving the system with no restoring force. Anyhow. note that the expansion of the RHS of Equation (2.10) is:

$$\frac{d^2}{dt^2}\delta R = \frac{G}{R_0^2}\left[\lambda\zeta(t) - M_{\text{eff}}\right] - \frac{2G}{R_0^3}\left[\lambda\zeta(t) - M_{\text{eff}}\right]\delta R. \tag{2.11}$$

Instantaneously, $\zeta(t)$ varies, so it can be written:

$$\lambda\zeta(t) = \lambda\langle\zeta\rangle + \lambda\left[\zeta(t) - \langle\zeta\rangle\right] \tag{2.12}$$
$$= \left[\lambda + \lambda\zeta(t) - \lambda\right] + \lambda\left[\zeta(t) - \langle\zeta\rangle\right] \tag{2.13}$$
$$= \left\{\lambda + \lambda\left[\zeta(t) - 1\right]\right\} + \lambda\left[\zeta(t) - \langle\zeta\rangle\right] \tag{2.14}$$
$$= M_{\text{eff}} + \lambda\left[\zeta(t) - 1\right], \tag{2.15}$$

substituting $\lambda\zeta(t) = M_{\text{eff}} + \lambda[\zeta(t) - 1]$ into the RHS of Equation (2.11), the first term simplifies to $G\lambda R_0^{-2}(\zeta - 1)$.

To illustrate the instability of time-averaged balance: For the δR term, use the time-averaged value $\lambda\langle\zeta\rangle = M_{\text{eff}}$ so the coefficient vanishes. Equation (2.11) is now:

$$\frac{d^2}{dt^2}\delta R = \frac{G\lambda}{R_0^2}\left[\zeta(t) - 1\right] - 0\cdot\delta R, \tag{2.16}$$

---

[5]$N = 100$ is large enough to say $M_{\text{eff}} \approx M_{\text{total}}$.
[6]The R^{-2} dependence as opposed to linear R prevents it from being a Mathieu equation, whose standard form is given in Equation.

since $\langle \zeta \rangle = 1$, the term in the brackets of 2.16 can be rewritten;

$$\frac{d^2}{dt^2} \delta R = \frac{G\lambda}{R_0^2} \left[\zeta(t) - \langle \zeta \rangle \right], \tag{2.17}$$

where there is no natural frequency. The ODE is now:

$$\frac{d^2}{dt^2} \delta R + \omega_0^2 \delta R = f(t), \tag{2.18}$$

which is the equation of a *forced undamped harmonic oscillator* with constant natural frequency,

$$\omega_0^2 = \frac{2G}{R_0^3} (\lambda - M_{\text{eff}}), \tag{2.19}$$

for $\lambda \approx M_{\text{eff}}$, $\omega_0^2 \approx 0$, indicating the system is near-critically balanced, making it susceptible to secular drift. When $\lambda < M_{\text{eff}}$, $\omega_0^2 < 0$, yielding complex frequencies and exponential instability rather than oscillations. Furthermore, the external driving term is:

$$f(t) = \frac{G\lambda}{R_0^2} \left[\zeta(t) - \langle \zeta \rangle \right]. \tag{2.20}$$

Since $\zeta(t) = 1 + \sin(\omega_\zeta t)$ and $\langle \zeta \rangle = 1$, inside the bracket of (2.20) becomes $\zeta(t) - \langle \zeta \rangle = \sin(\omega_\zeta t)$;

$$f(t) = \frac{G\lambda}{R_0^2} \sin(\omega_\zeta t). \tag{2.21}$$

The general solution to the forced harmonic oscillator in Equation (2.18) looks like:

$$\delta R(t) = \left[C_1 \cos(\omega_0 t) + C_2 \sin(\omega_0 t) \right] + \frac{G\lambda}{R_0^2 \left(\omega_0^2 - \omega_\zeta^2 \right)} \sin(\omega_\zeta t), \tag{2.22}$$

where the bracket term is the homogeneous solution and the last term is a particular solution. The particular solution is derived using the method of undetermined coefficients for a forced harmonic oscillator; it has amplitude,

$$\delta R_{\text{amp}} = \frac{G\lambda}{R_0^2 \left(\omega_0^2 - \omega_\zeta^2 \right)}. \tag{2.23}$$

When $\omega_0 \approx \omega_\zeta$, the driving term synchronizes with the system's natural oscillation frequency, causing each cycle to add energy coherently, resulting in resonant amplification where oscillation amplitudes grow without bound in the linear approximation. [7]

2.3 Energy Analysis

The total energy of the system is:

$$E_{\text{total}}(t) = T + V_{\text{grav}} + V_\zeta(t), \tag{2.24}$$

where the kinetic and potential energies terms are,

$$T = \frac{1}{2} \sum_{i=1}^{N} m_i v_i^2 \tag{2.25}$$

$$V_{\text{grav}} = -\frac{1}{2} \sum_{i \neq j} \frac{G m_i m_j}{r_{ij}^2 + \varepsilon_{\text{grav}}^2} \tag{2.26}$$

---

[7]The velocity Verlet integrator accurately tracks this energy injection with minimal numerical error if a small enough Δt is used.

$$V_\zeta(t) = +\frac{1}{2}\sum_{i\neq j}\frac{\lambda G\zeta(t)}{r_{ij}^2 + \varepsilon_\zeta^2}\,. \tag{2.27}$$

Since $\zeta(t)$ is time-dependent, the system is *non-concentrative*; the work done by the time-varying repulsive force over one period with frequency ω_ζ is:

$$W_\zeta = \oint \vec{F}_\zeta(t)\,\vec{dr}, \tag{2.28}$$

where the closed integral would be zero if the system was conservative, otherwise, energy accumulates and the system secularly expands or contracts without stable oscillations.

2.3.1 Adiabatic Invariance Violation

An adiabatic invariant is a quantity that remains approximately constant when the parameters governing a cyclical physical system are altered very slowly relative to the system's natural frequency of motion. This concept is distinct from the thermodynamic definition of an adiabatic process, focusing instead on the rate of change of the environment.[8] The action variable is the adiabatic invariant for any harmonic oscillator;

$$\eth = \frac{E}{\omega_0}\,. \tag{2.29}$$

When $\omega_0 \approx \omega_\zeta$ and the driving frequency matches the natural frequency, the system cannot adiabatically follow the modulation; instead, energy couples coherently into the oscillation with each cycle. Each drive cycle adds energy resonantly rather than averaging out, violating the invariance and causing resonant energy pumping.

For stability, the natural frequency ω_0 must be sufficiently detuned from the driving frequency ω_ζ to prevent resonant energy coupling. Systems operating near resonance ($\omega_0 \approx \omega_\zeta$) experience unbounded growth due to coherent phase-matching between the oscillation and the drive. Conversely, when $\omega_0 \ll \omega_\zeta$ or $\omega_0 \gg \omega_\zeta$, the system responds adiabatically to the modulation, averaging over multiple drive cycles without energy accumulation.

2.3.2 Virial Theorem Considerations

The system used here includes a time-varying repulsive force that requires a generalized virial theorem as opposed to a standard virial theorem which is used for self-gravitating systems states in equilibrium. The general virial equation is:

$$\frac{d^2 I}{dt^2} = 4T - \sum_i \vec{r}_i \cdot \vec{F}_i, \tag{2.30}$$

where $I = \sum_i m_i r_i^2$ is the moment of inertia and r_i is the scalar distance of particle i from the center of mass of the system.

---

[8]A classic example is the action variable in mechanics: As external parameters like system energy, kinetic energy, or potential energy change slowly over time, the action remains invariant, proving to be a useful tool for understanding stability in systems like planetary orbits or confined plasma particles.

3 Empirical Stability Scan

Appendix A: Energy Errors and Time Reversibility

A.1   How Velocity Errors Affect Energy Errors

The laws of motion for conservative physical systems are time-reversible. If the system is ran forward in time such that $t_{\ell+1} = t_\ell + \Delta t$, and then ran backward using the same exact method and timestep, the ending should match the start. Time-irreversibility causes phase space area to drift away from its true value in an uncontrolled manner; in turn, certain physical properties may not be preserved by the unstable simulation. The relationship between velocity errors and energy errors, and the fact that certain numerical integration methods like Verlet integration conserve energy well, are fundamentally connected to the time-reversibility of Hamiltonian systems.

$$H(\vec{r}, \vec{p}) = T(\vec{v}) + V(\vec{r}) = \frac{1}{2}m|\vec{v}|^2 + V(\vec{r}), \tag{A.1}$$

where $\vec{p}$ is the momentum and $H(\vec{r}, \vec{p}) = E_{\text{total}}$ is the Hamiltonian of a conserved dynamical system. Anyhow,

$$\dot{H}(\vec{r}, \vec{p}) = m\vec{v} \cdot \dot{\vec{v}} + \nabla V \cdot \dot{\vec{r}}. \tag{A.2}$$

Recall Newton's second law and that using $\vec{F} = -\nabla V$,

$$\dot{H}(\vec{r}, \vec{p}) = \vec{v} \cdot \vec{F} - \vec{F} \cdot \vec{v} = 0, \tag{A.3}$$

it has been shown that energy is conserved exactly in continuous dynamics here. Even in non-conserved systems, velocity errors affect the instantaneous mechanical energy because $T(\vec{v})$ depends quadratically on velocity, so any deviation in $\vec{v}$ directly alters $H = T + V$, regardless of whether total energy is conserved over time. Energy error refers to whether your numerical method accurately computes H at each step; so even if E_{total} is not conserved as $H = H(t)$, energy errors can still exist if the calculation for $\vec{v}$ is off. Non-conserved systems do not eliminate energy error, they change accuracy of the instantaneous mechanical energy. In a non-conserved system, it is not tracked whether energy stays constant, but whether the integrator properly follows whether the integrator accurately tracks the instantaneous mechanical energy over time. Even when energy is not conserved, velocity errors can distort the systems true dynamics, making accurate tracking of instantaneous mechanical energy essential for physical fidelity.

Regarding numerical error propagation: If the velocity has an error $\delta\vec{v}$, then the kinetic energy error is:

$$\delta T = \frac{1}{2}m|\vec{v} + \delta\vec{v}|^2 - \frac{1}{2}m|\vec{v}|^2 \tag{A.4}$$

$$= m(\vec{v} \cdot \delta\vec{v}) + \frac{1}{2}m|\delta\vec{v}|^2. \tag{A.5}$$

For small errors, $|\delta\vec{v}|^2 \ll \vec{v} \cdot \delta\vec{v}$; for that reason, an approximation for kinetic energy can be obtained by discarding the higher-order term:

$$\delta T \approx m\vec{v} \cdot \delta\vec{v}. \tag{A.6}$$

Because $\delta T \propto |\delta\vec{v}|$, velocity errors directly translate to energy errors. Although energy conservation in physical systems does not *automatically* translate to numerical stability in simulations, numerical stability comes from using an integration method that respects the underlying mathematical structure of the physical system, which includes properties like time reversibility and energy conservation.

A.2   Time-Reversibility of Certain Integration Methods

A.2.1   Explicit Euler Method (irreversible)

The explicit Euler method advances the state based on standard kinematic equations of motion;

$$x_{\ell+1} = x_\ell + v_\ell\Delta t \tag{A.7}$$

$$v_{\ell+1} = v_\ell + a_\ell\Delta t. \tag{A.8}$$

The above formulas step forward from t_ℓ to $t_{\ell+1}$ which are Δt apart. Rearrange them to go backward in time from $t_{\ell+1}$ to t_ℓ;

$$x_\ell = x_{\ell+1} - v_\ell \Delta t \tag{A.9}$$

$$v_\ell = v_{\ell+1} - a_\ell \Delta t . \tag{A.10}$$

So when at $t_{\ell+1}$, to know the state at time t_ℓ, v_ℓ and a_ℓ must already be known, which goes against the very reason it was started.

A.2.2 Basic Størmer–Verlet Algorithm (reversible)

The Verlet algorithm is a second-order method that relies on the state at the current time and the state of the time point that is one timestep behind t_ℓ to find the state at $t_{\ell+1}$. The second-order differential equation is:

$$x_{\ell+1} = 2x_\ell - x_{\ell-1} + a_\ell \Delta t^2 . \tag{A.11}$$

Starting at $t_{\ell+1}$ and going backward to $t_{\ell-1}$,

$$x_{\ell-1} = 2x_\ell - x_{\ell+1} + a_\ell \Delta t^2 , \tag{A.12}$$

which is possible since the state at one time point before $t_{\ell+1}$ is known in the Størmer method.

A.2.3 Classic Runge–Kutta Method (irreversible)

The classic Runge–Kutta method (RK4) is a fourth-order method that can solve a wide range of initial value ordinary differential equations without being tailored to a specific type of problem. To calculate $x_{\ell+1}$:

$$x_{\ell+1} = x_\ell + \frac{\Delta t}{6} \left(\kappa_1 + 2\kappa_2 + 2\kappa_3 + \kappa_4 \right) , \tag{A.13}$$

where the κ values are the intermediate steps whose quantities depend on $f(t,x) = \dot{x}$ such that:

$$\kappa_1 = f\left(t_\ell, x_\ell\right) \tag{A.14}$$

$$\kappa_2 = f\left(t_\ell + \frac{\Delta t}{2}, x_\ell + \frac{\kappa_1 \Delta t}{2}\right) \tag{A.15}$$

$$\kappa_3 = f\left(t_\ell + \frac{\Delta t}{2}, x_\ell + \frac{\kappa_2 \Delta t}{2}\right) \tag{A.16}$$

$$\kappa_4 = f\left(t_\ell + \Delta t, x_\ell + \kappa_3 \Delta t\right) . \tag{A.17}$$

This formulation of κ means that there is no standard formula that simply reverses the forward step. This asymmetry is ultimately the reason for drift. RK4 methods offer improved accuracy through multiple force evaluations per timestep, though they are not symplectic and thus do not guarantee the same level of energy stability as Verlet-family integrators.

Appendix B: Truncation Error Analysis via Taylor Expansion

The Taylor series expansion of $\vec{r}(t+\Delta t)$ about t is,

$$\vec{r}_{\text{exact}}(t+\Delta t) = \vec{r}(t) + \dot{\vec{r}}(t)\Delta t + \frac{1}{2}\ddot{\vec{r}}(t)\Delta t^2 + \frac{1}{6}\dddot{\vec{r}}(t)\Delta t^3 + \mathcal{O}(\Delta t^4). \tag{B.1}$$

The Euler approximation is,

$$\vec{r}_{\text{Euler}}(t+\Delta t) = \vec{r}(t) + \vec{v}(t)\Delta t, \tag{B.2}$$

so the leading error term is $\frac{1}{2}\ddot{\vec{r}}(t)\Delta t^2$; therefore, the local error is $\mathcal{O}(\Delta t^2)$. Similarly, the Verlet approximation is,

$$\vec{r}_{\text{Verlet}}(t+\Delta t) = \vec{r}(t) + \vec{v}(t)\Delta t + \frac{1}{2}\vec{a}(t)\Delta t^2, \tag{B.3}$$

with the leading error and local error being $\frac{1}{6}\dddot{\vec{r}}(t)\Delta t^3$ and $\mathcal{O}(\Delta t^3)$ respectively. Moreover, global errors are the accumulation of local errors over the time of simulation: $n = t_{\text{final}}/\Delta t$, where n would be the number of timesteps iterated by the simulation. For the Euler method: $n \times \mathcal{O}(\Delta t^2) = (t_{\text{final}}/\Delta t) \times \mathcal{O}(\Delta t^2) \to \mathcal{O}(\Delta t)$. Similarly, for Verlet integration: $n \times \mathcal{O}(\Delta t^3) = (t_{\text{final}}/\Delta t) \times \mathcal{O}(\Delta t^3) \to \mathcal{O}(\Delta t^2)$.

Appendix C: Virial Theorem

The virial theorem implies that the inward pull of gravity is countered by the outward motion of particles. If a system satisfies this balance, it is in a stable, bound state. If it violates this balance—e.g., the particles are moving too fast— the system will expand; but if they are moving too slow, then gravity will collapse it inward. For N-body simulations, the Virial theorem is a handy tool. Both the kinetic and potential energy can be computed at each timestep and check whether they maintain the expected ratio, which by standard is expected be $V_{\mathrm{grav}} = -2T$. Deviations from the expected ratio indicate whether the system is drifting out of equilibrium or whether your numerical integration is introducing systematic errors and can also be helpful for setting initial conditions. The classical virial theorem only works for time-independent, conservative systems. In time-dependent systems such as those proposed in this letter, to relate the kinetic energy of a system to the forces acting on its constituent particles the generalized virial theorem is used.

C.1 Derivation of Generalized Formula

For a system of N particles with masses m_i and position vectors $\vec{r}_i$, define the *scalar moment of inertia*:

$$I = \sum_{i=1}^{N} m_i r_i^2, \tag{C.1}$$

then take its first derivative with respect to time:

$$\frac{d^2 I}{dt} = \sum_i m_i \frac{d}{dt}(\vec{r}_i \cdot \vec{r}_i) \tag{C.2}$$

$$= \sum_i m_i (2 \vec{r}_i \cdot \dot{\vec{r}}_i) \tag{C.3}$$

$$= 2 \sum_i m_i \vec{r}_i \cdot \vec{v}_i, \tag{C.4}$$

and the second derivative:

$$\frac{d^2 I}{dt^2} = 2 \sum_i m_i \frac{d}{dt}(\vec{r}_i \cdot \vec{v}_i) \tag{C.5}$$

$$= 2 \sum_i m_i (\vec{v}_i \cdot \vec{v}_i + \vec{r}_i \cdot \dot{\vec{v}}_i) \tag{C.6}$$

$$= 2 \sum_i m_i v_i^2 + 2 \sum_i m_i \vec{r}_i \cdot \vec{a}_i \tag{C.7}$$

$$= 2 \sum_i m_i v_i^2 + 2 \sum_i \vec{r}_i \cdot \vec{F}_i. \tag{C.8}$$

Moreover, since the total kinetic energy is, $T = \sum_i \frac{1}{2} m_i v_i^2$;

$$\sum_i m_i v_i^2 = 2T, \tag{C.9}$$

substituting this into Equation (C.8) yields:

$$\frac{d^2 I}{dt^2} = 4T - \sum_i \vec{r}_i \cdot \vec{F}_i, \tag{C.10}$$

this is the generalized virial theorem in its exact form.

C.2 Time-Averaged Form

For systems in quasi-equilibrium (periodic motion without secular drift), time-averaging over a period τ gives:

$$\left\langle \frac{d^2 I}{dt^2} \right\rangle = \frac{1}{\tau} \int_0^\tau \frac{d^2 I}{dt^2} dt = \frac{1}{\tau} \left[\frac{dI}{dt} \bigg|_\tau - \frac{dI}{dt} \bigg|_0 \right]. \tag{C.11}$$

For periodic motion, $\frac{dI}{dt}$ returns to its initial value; thus, $\left\langle \frac{d^2 I}{dt^2} \right\rangle = 0$. This yields the time-averaged virial condition:

$$2\langle T \rangle = \left\langle \sum_i \vec{r}_i \cdot \vec{F}_i \right\rangle. \tag{C.12}$$

C.3 Application to Homogeneous Potentials

For conservative forces derivable from a potential $V(\vec{r}_1, \ldots, \vec{r}_N)$, $\vec{F}_i = -\nabla_i V$. For V to be a *homogeneous function of degree v*, it must satisfy,

$$V(\tilde{\gamma}\vec{r}_1, \ldots, \tilde{\gamma}\vec{r}_N) = \tilde{\gamma}^v V(\vec{r}_1, \ldots, \vec{r}_N). \tag{C.13}$$

Anyhow, define $\tilde{\gamma}$ such that:

$$\Upsilon(\tilde{\gamma}) = V(\tilde{\gamma}\vec{r}_1, \ldots, \tilde{\gamma}\vec{r}_N), \tag{C.14}$$

then, take the derivative of V with respect to $\tilde{\gamma}$;

$$\frac{d}{d\tilde{\gamma}}\Upsilon(\tilde{\gamma}) = \sum_{i=1}^{N} \nabla_i V(\tilde{\gamma}\vec{r}_1, \ldots, \tilde{\gamma}\vec{r}_N) \cdot \frac{d}{d\tilde{\gamma}}(\tilde{\gamma}\vec{r}_i) \tag{C.15}$$

$$= \sum_{i=1}^{N} \nabla_i V(\tilde{\gamma}\vec{r}_1, \ldots, \tilde{\gamma}\vec{r}_N) \cdot \vec{r}_i, \tag{C.16}$$

but from the homogeneity condition in (C.13):

$$\Upsilon(\tilde{\gamma}) = \tilde{\gamma}^v V(\vec{r}_1, \ldots, \vec{r}_N) \quad \Rightarrow \quad \frac{d}{d\tilde{\gamma}}\Upsilon(\tilde{\gamma}) = v\tilde{\gamma}^{v-1} V(\vec{r}_1, \ldots, \vec{r}_N). \tag{C.17}$$

Now evaluate at $\tilde{\gamma} = 1$:

$$\sum_{i=1}^{N} \nabla_i V(\vec{r}_1, \ldots, \vec{r}_N) \cdot \vec{r}_i = vV(\vec{r}_1, \ldots, \vec{r}_N), \tag{C.18}$$

or, more cleanly

$$\sum_{i=1}^{N} \vec{r}_i \cdot \nabla_i V = vV. \tag{C.19}$$

C.3.1 Euler's Homogeneous Function Theorem

The steps to obtain Equation (C.19) are roughly a form of proof of Eulers theorem for homogeneous functions, which states that if a scalar function $s(\vec{r})$ is homogeneous of degree v, meaning,

$$s(\tilde{\gamma}\vec{r}) = \tilde{\gamma}^v s(\vec{r}) \qquad \forall \tilde{\gamma} > 0, \tag{C.20}$$

then,

$$\vec{r} \cdot \nabla s(\vec{r}) = v s(\vec{r}). \tag{C.21}$$

C.3.2 Standard Form of Virial Theorem

For time-averaged equilibrium with homogeneous potentials:

$$2\langle T \rangle = -v\langle V \rangle. \tag{C.22}$$

For gravitational potentials, $V_{\text{grav}} \propto r^{-1}$, so $v = -1$;

$$2\langle T \rangle = -\langle V_{\text{grav}} \rangle. \tag{C.23}$$

For harmonic potentials on the other hand, $V_{\text{harmonic}} \propto r^2$ and so $v = 2$,

$$\langle T \rangle = \langle V_{\text{harmonic}} \rangle. \tag{C.24}$$